Supporting Information for:

Environmental aspects of use of recycled carbon fibre composites in automotive applications

Fanran Meng[†], *Jon McKechnie*[†,*], *Thomas Turner*[†], *Kok H Wong*[‡], *Stephen J Pickering*[†]

† Department of Mechanical, Materials and Manufacturing Engineering, University of Nottingham, Nottingham NG7 2RD, UK

‡ Department of Science and Engineering, University of Nottingham, Taikangeast Road No.199, Ningbo, China

[*] *Corresponding author: Email address: Jon.Mckechnie@nottingham.ac.uk*

The supporting information contains 20 pages, including 1 tables and 6 figures.

1 METHOD

The goal of this study is to assess the life cycle environmental impacts of carbon fibre reinforced polymer (CFRP) recycling and use of recovered carbon fibre (rCF) for composite manufacture for automotive applications. Details of process models of rCF processing and recycled CFRP (rCFRP) manufacture are presented in this supplementary information.

Activities included within the life cycle model are shown in Figure S1, beginning with collected CFRP waste and including all subsequent activities related to CFRP recycling, rCF processing, rCFRP manufacture, and use phase. rCF is assumed to be recovered from a fluidised bed recycling process. rCF is either processed into non-woven mat or aligned mat before compression moulded or injection moulded into final rCFRP products. Production of rCFRP is also compared with similar components produced from virgin carbon fibre (vCF) as shown in Figure S1.

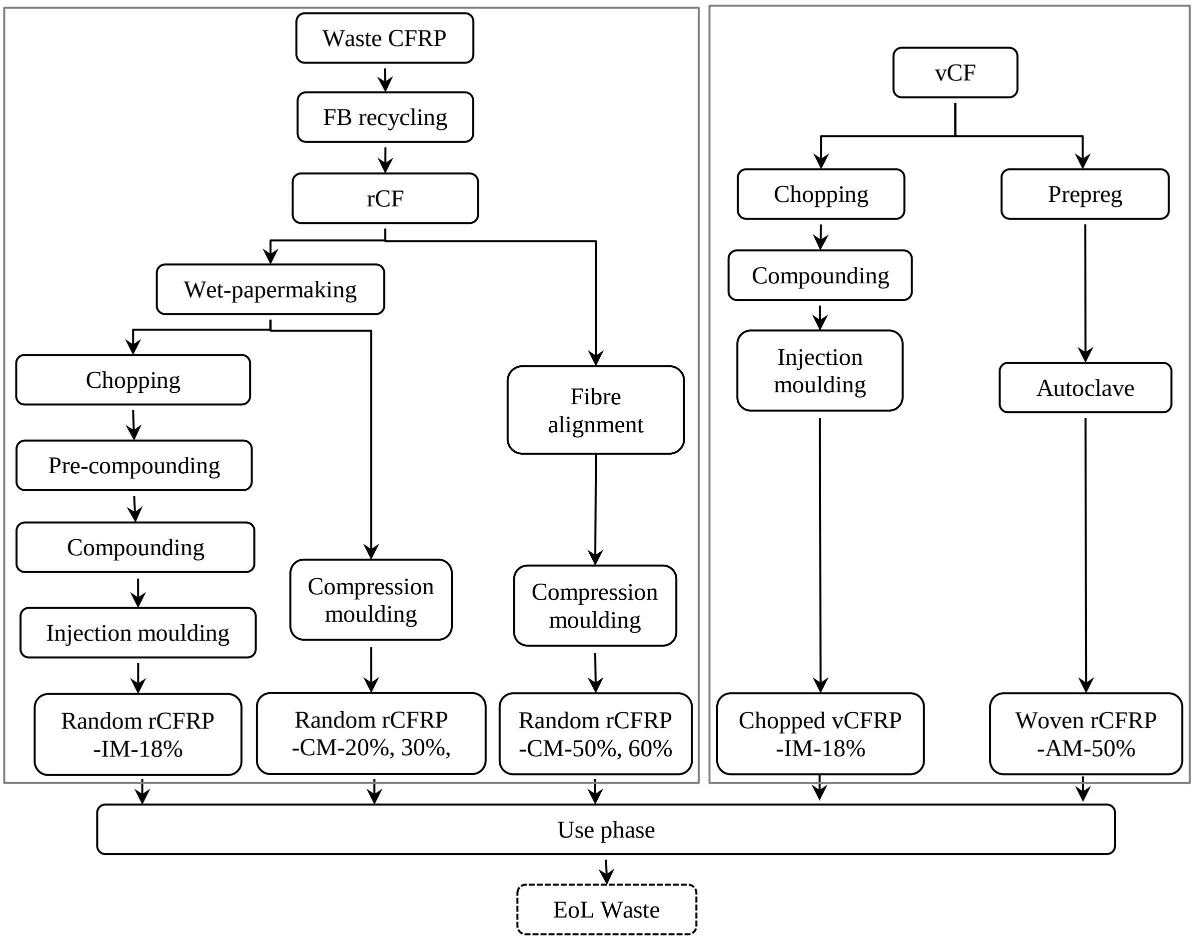

Figure S1. Overview of pathways and processes for manufacture of automotive components from recycled and virgin carbon fibre.

1.1 Fibre alignment

A fibre alignment process consists of fibre dispersion, alignment, and comingling with resin to form a fibre mat as shown in Figure S2.[1] Discontinuous rCF from the fluidised bed process is dispersed in a aqueous liquid to form a fibre suspension. The suspension is then sprayed onto a mesh screen inside a rotating drum, which filters the fibre dispersion to separate the CF. Vacuum suction is employed beneath the mesh to accelerate the dewatering step. The width of the fibre mat is controlled by the range of the nozzle movement with a linear actuator. After steam washing, the mat is later subjected to an epoxy based binder application via vacuum drying and thermal drying as in the papermaking process described previously.

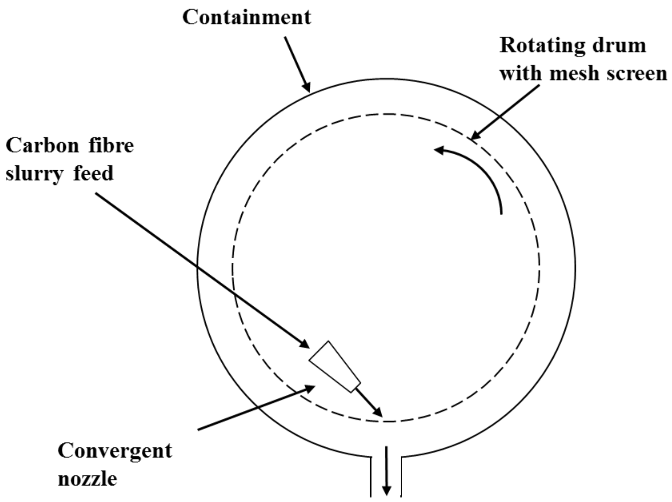

Figure S2. A diagram of the fibre alignment process rig.

1.2 CFRP manufacture

1.2.1 Manufacture of CFRP via compression moulding

Compression moulding production of CFRP from rCF and vCF requires a set of process steps. Before applying compression pressure, a standard vacuum bagging procedure is implemented to reduce air entrapment during ply collation and thus to reduce the void content inside the composite.[2] Energy consumption for vacuum bagging can be obtained from literature.[3] Energy requirements of compression moulding consist of thermal energy and kinetic energy and are modelled based on the characteristics of standard equipment and required moulding pressure. For random rCFRP, the mould is subsequently compressed under pressure of 2 to 14 MPa depending on fibre volume fraction (vf) required, with higher fibre fraction components requiring higher pressures.[2] For aligned rCFRP, high vf requires relatively lower compression pressure (8 MPa).[4]

The thermal energy required for the moulding process is calculated based on temperature profile, heat capacity of materials/equipment and estimated heat losses. In the heating stage, the energy is to heat the charge to the moulding temperature. In the curing stage, the energy supply is equal to heat losses of the mould. To simplify the development of the model, conductive heat loss is assumed to be negligible. Thus there is only convective and radiative heat loss from the moulding system. Energy inputs are assumed to be delivered by electric heating as described before.

Kinetic energy is required to compress the mats at required pressure. Compression is assumed to be provided by hydraulic press and energy requirements are calculated based on the force/ process pressure required for compression and component thickness. Energy consumption is assumed to be in the pressure applying stage. A machine's capacity (*F*) is a function of the moulding force for the parts. It includes excess capacity and a 25% safety factor beyond the force required. Equipment-specific parameters such as the pressing speed, pressure ramp rate and ram area can be used for calculation of kinetic energy (Q_k). It can be calculated as below where efficiency of applying pressure is assumed to be 100%:[5]

$$\mathrm{Q}_k = (pA - p_a A_0) v \frac{p}{\dot{p}} \tag{1}$$

Where A is the part's projected area (m^2), p is the compression moulding pressure (MPa) based on vf required, A_0 is the ram area (m^2), v is the pressing speed depending on the machine selected (m/s), p_a is the ambient pressure (MPa), $\dot{p}$ is the pressure ramp rate(MPa/s).

The remaining energy consumption for the finishing step and cooling step are assumed to be 1.2 MJ/kg[6] and 0.90MJ/kg,[7] respectively, which gives a total energy consumption of compression moulding is 14.4 MJ/kg for manufacture rCFRP with 20% vf. Energy requirements for compression moulding are not strongly related to the component thickness as discussed in previous work.[8].

1.2.1.1 Validation

The energy requirement of compression moulding process has been reported to be 7.2-13.05 MJ/kg [6, 9] for composites. To accommodate for rCF manufacture process to obtain the mechanical properties assumed in this study, an additional vacuum bagging procedure (approximately 35% of total energy consumption) was implemented for 30 mins at room temperature before applying the compression pressure to reduce the void content as in previous work[2]. Therefore, energy consumption of the compression moulding of rCFRP is slightly higher than normal.

1.2.2 Manufacture of CFRP via injection moulding

1.2.2.1 Compounding energy calculation

Energy requirements for the compounding process are calculated accounting for polymer melting, screw driving, and cooling and combined with the output of the compounder as shown in eq 2 below. With energy consumption and output of compounding process, specific energy requirement can be calculated.

$$E_{total} = E_{melt} + P_{plasticizing} t_p + P_{cool} t_c \tag{2}$$

Where E_{melt} is the energy used to meld the resin (MJ), $P_{plasticizing}$ is the energy to drive the screw (MJ), t_p is plasticizing time to melt and deliver them for injection (s), P_{cool} is the energy used to cool the mould to return it to a solid state (kW), t_c is cooling time required to cool the polymer to a temperature to solidify within the mould (s).

The energy needed to melt the polymer varies according to the crystalline nature of the polymer and as PP is a crystalline polymer, it can be expressed in eq 3 below:[10]

$$E_{melt} = mc_p(T_{mel} - T_a) + \lambda m H_F \tag{3}$$

Where c_p is the specific heat capacity of the polymer (J/(kg·K)), m is the mass of injection shot (kg), T_a is the ambient temperature (K), T_{mel} is the melting temperature of the polymer (K), λ is the degree of crystallization, for PP, λ is assumed to be 60%, H_F is the heat of fusion for 100% crystalline polymer (kJ/kg).

The rotary driving unit of the rotating screw plays an important role in compounding machines. Screw torque and rotational speed convey the polymer and provide the recommended level of shear and homogenization.[11] Rotational speed to process rCF and polypropylene into injection moulded pellets are obtained from previous experimental work.[12] The dissipated power at a given speed can then be calculated using the torque and the rotational speed of the screw. Based on the screw diameter and L/D_s ratio selected for injection, key dimensions of screws for processing can be determined accordingly.[11] The forward channel velocity can be calculated based on the rotation speed and dimensions of the screw as below. As the length of the screw has been determined by the L/D_s ratio of the selected injection moulding machine, the residence time for plasticizing (t_p) can thus be estimated. [13]

$$v = \frac{\pi N D_s}{60} cos\theta \tag{4}$$

Where N is the screw rotational speed (rpm), θ is the helix angle ($\theta = \tan^{-1}\frac{t}{\pi D_b}$) (°), t is the pitch (t=D_s) (mm), D_b is the diameter of the barrel diameter (D_b=D_s+2H) (mm), H is the channel depth (mm), D_s is the screw diameter (mm).

There are chiller units for the water cooling mechanism that circulates around the barrel. The cooling power consumption in this study can be simplily estimated by a linear relationship between cooling power and compounding power[14] while the residence time for compounding process is obtained from previous experiments.[12]

The output (*kg/hr*) of the compounder can be obtained from a flow rate function of the conveying efficiency and the feed depth and simulating the impact of these factors on the flow rate.[15]

1.2.2.2 Injection moulding energy calculation

Energy requirement of injection moulding is modelled based on standard equipment applied to particular materials. Energy requirements for various hydraulic injection moulding machines have been reported in several studies.[10, 16-23] The total energy requirement for an injection moulding machine consists of melting and injecting resin and additional sub-process energy for opening, closing and ejecting mould and the clamping action, as shown in eq 5.

$$E_{total} = E_{melt} + P_{plasticizing}t_p + E_{injection} + P_{cool}t_c + E_{reset} \tag{5}$$

Where E_{melt} is the energy used to melt the resin (MJ) and is calculating as described above in eq. 3, $P_{plasticizing}$ is the energy used to drive the screw during the period for plasticizing (kW), t_p is plasticizing time to melt and deliver them for injection (s), $E_{injection}$ is the energy required to inject the molten polymer (MJ), P_{cool} is the energy used to cool the mould to return it to a solid state (kW), t_c is cooling time required to cool the polymer to a temperature to solidify within the mould (s), E_{reset} is the resetting energy, including the energy consumed to hold the mould during injection, the energy needed to open and close the mould and to eject the part from the mould (MJ). E_{melt} and $\mathrm{P}_{plasticizing}$ can be calculated using the same way as in compounding process.

Recommended processing data for injection moulding process of CF-PP are obtained from previous experiments:[12] injection temperature is 210 °C, ejection temperature is 88 °C, mould temperature is 50 °C, injection pressure is 120-160 MPa and rotational speed is 125 rpm. Using the processing data, injection moulding machine can be selected based on clamping force accordingly. [24, 25]

The energy required to inject the molten polymer to the mould can be calculated by summing the injection pressure ($p_{injection}$) multiplied by the volume of the cavity ($V_{injection}$) as shown in eq 6 below:[10]

$$E_{injection} = \frac{p_{injection}V_{injection}}{\eta_{eff}} \tag{6}$$

Where η_{eff} is 80% which is within the efficiency interval of the injection machines found in literature.[19]

Injection moulding machines are able to achieve the required flow rate for injection with the injection units. During the injection stage, the full injection power is assumed to be utilized and the recommended injection pressure is achieved. Because of the flow resistance in the mould channels and the channel shrinkage from solidification of polymer against the walls, the flow rate reduces from the maximum value in the filling stage. Therefore, injection moulding time can be calculated based on the average flow rate using eq 7.[26]

$$t_i = 2V_s p_i / P_i \tag{7}$$

Where P_i is injection power (kW), p_i is recommended injection pressure for a specific polymer (kPa), V_s is the required shot size (m^3).

In the injection system, there are chiller units for the water cooling mechanism that circulates around the barrel. The cooling power consumption in this study can thus be simplily estimated by a linear relationship between cooling power and injection machine power, which is 10.4 kW for a 165 kW machine.[14, 19] The relationship between cooling time and the central temperature of the mould is given below: [26]

$$t_c = \frac{{h_{max}}^2}{\pi^2 \alpha} ln \frac{4(T_i - T_{mol})}{\pi(T_x - T_{mol})} \tag{8}$$

Where h_{max} is the part thickness (mm), α is thermal diffusivity coefficient (mm^2/s), T_i is the polymer injection temperature (K), T_x is the recommended ejection temperature (K), T_{mol} is the recommended mould temperature (K).

The resetting energy is the sum of energy to open and close the mould and to eject the part, accounting for about 25% of the energy consumed in the total process.[20, 22] Resetting time is defined as the sum of time required to open and close the mould and eject the part from the cavity:[26]

$$t_r = 1 + 1.75 t_d \left(\frac{2D + 5}{L_s}\right)^{1/2} \tag{9}$$

Where t_d is the dry cycle time (s), D is the part depth (mm), L_s is the maximum clamping stroke (mm).

1.2.2.3 Validation

The injection moulding cycle time and total energy consumption value have been compared with literature values (2.0-7.9 MJ/kg composites) to ensure the model is representative.[11, 18, 27-30] Cooling time dominates the injection moulding process (>50% of the total time) and the resin melting step consumes the majority of the total moulding process energy, although the energy values vary depending on processing specifications (e.g., injection temperature) and part geometry.

1.3 Functional unit

The functional unit chosen for this study is a generic automotive component, assumed to be produced from mild steel. When evaluating alternative materials, functional equivalence is maintained by considering the design material index (λ) and varying component thickness to account for differences in each material's mechanical properties. Properties of vCFRP and random rCFRP were obtained from the previous experiments[2] and manufacturers,[31, 32] properties of aligned rCFRP were calculated using a micromechanics model for CFRP properties[33, 34] while data for other engineering materials is taken from online database[35-37] as shown in Table S1. Component dimensions are input to the CFRP manufacturing models to ensure material-specific part geometries are considered in the analysis.

Table S1. Material properties of general engineering materials selected for LCA study

Material	Matrix	Manufacture	Density, g/cm3	Modulus, GPa	Strength, MPa	References
Mild steel	-	Stamping	7.81	207	350	[35]
Magnesium	-	Die-casting	1.81	45	150	[36]
Aluminium	-	Wrought	2.70	69	276	[37]
Random rCF 20%	Epoxy resin	Compression moulding	1.32	27.6	260	[2]
Random rCF 30%	Epoxy resin	Compression moulding	1.38	37.1	341	[2]
Random rCF 40%	Epoxy resin	Compression moulding	1.44	39.8	302	[2]
Aligned rCF 50%	Epoxy resin	Compression moulding	1.50	60.8	-	calculated
Aligned rCF 60%	Epoxy resin	Compression moulding	1.56	73.9	-	calculated
Woven vCF 50%	Epoxy resin	Autoclave moulding	1.6	70	570	[32]
Random rCF 18%	PP	Injection moulding	1.17	16.3	125	[4]
Chopped vCF 18%	PP	Injection moulding	1.07	16.2	117	[31]

2 RESULTS

2.1 Component manufacture analysis

The normalised production PED associated with raw material and part manufacture is shown in Figure S4. Similar with global warming potential results (see Figure 1 in the main text), the results show production PED decreases with the increasing vf for compression moulding pathways of rCFRP. This can be attributed to PED reduction from the reduced content of epoxy resin mitigating the increase of PED associated with the CF recycling and manufacturing, whereby 1 kg epoxy resin of 138 MJ versus 1 kg rCF of 35 MJ for rCF recycling and manufacturing.

In the injection moulding pathways, rCFRP component with 18% rCF volume fraction shows lower normalised PED requirement of 2.39 MJ/part while the vCFRP component presents quite high normalised PED burdens primarily due to the high environmental impacts of vCF manufacture (10.27 MJ/part).

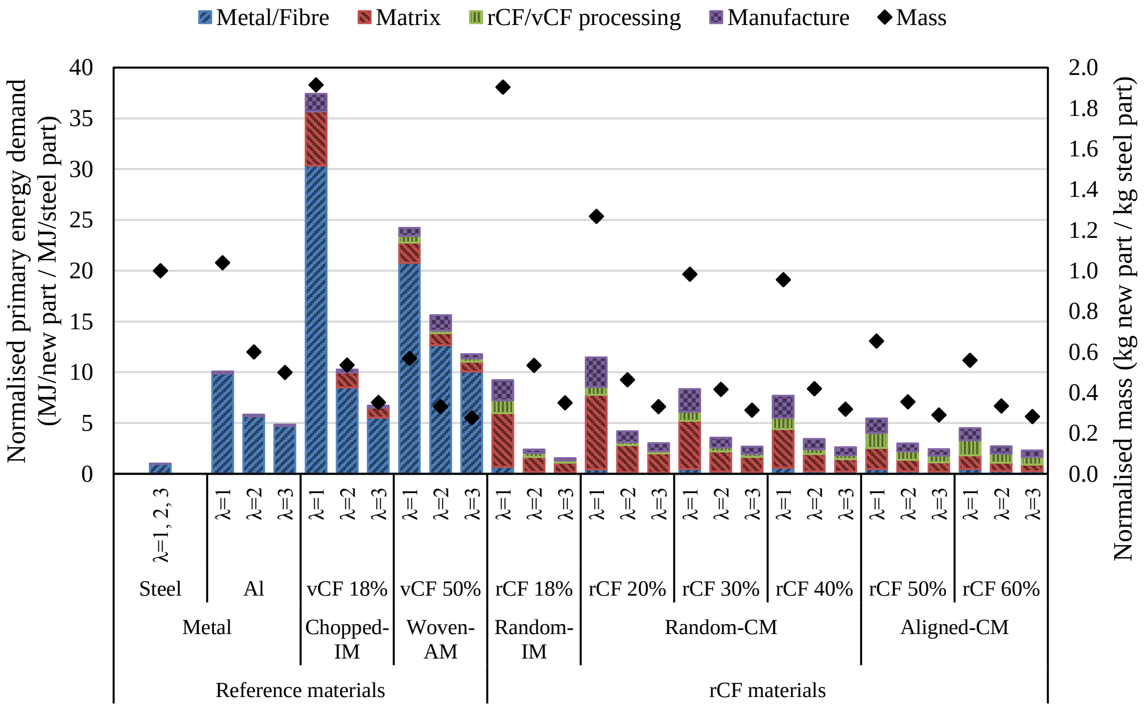

Figure S3. Normalised production PED (MJ/new part relative to MJ/steel part) and mass (kg new part relative to kg steel part) of components achieving equivalent stiffness for material design constraint λ=1, 2 , 3.

2.2 Sensitivity analysis

Uncertainty associated with vCF production impacts arise from data quality issues as well as regional variability of electricity generation sources and associated impacts. Due to the low GHG intensity of 7 g CO_2eq. per kWh electricity produced from hydro power, 1 kg vCF production only emits 29 kg CO_2eq. compared to 68 kg CO_2eq. using coal electricity source of which the GHG intensity is 960 g CO_2eq. per kWh (see Figure S5). With the highest electricity intensity, the GHG emission of rCF production would be only up to 9% of vCF production compared to 5% using UK electricity mix. Since vCF production has a high energy intensity and the renewable electricity content affects the GHG emissions of vCF manufacture, more and more industries are seeking sustainable and low cost energy sources such as SGL Automotive Carbon Fibres and BMW group set up the vCF production process in Moses Lake, USA to use 100% hydro power electricity for BMW I series car manufacture. [38 38 38 38 38 38 38] On the other hand, this result indicates markets for rCF– potential trade-off between environmental impact reductions in recycling and providing the same functional requirement with vCF.

The quality of life cycle inventory data for vCF manufacture is poor: publicly available data is limited; vCF production energy requirement and sources vary significantly (198 to 595 MJ/kg from a mix of electricity, natural gas, and steam);[9, 39-41] and studies have not linked production data to CF properties despite different processing conditions required to achieve high modulus and high strength CF (between 1000-1400°C for high modulus fibers, or 1800-2000°C for high strength fibers). Therefore, there is inadequate information to match energy intensity to fibre properties. But the impact of various literature values on life cycle results are assessed in low case (198 MJ/kg) and high case (595 MJ/kg) relative to the base case developed based on the literature (149.4 MJ electricity, 177.8 MJ natural gas and 31.4 kg steam per kg vCF) (see shaded area in Figure S5). The same ratio of energy types (electricity, natural gas and steam) is assumed for low and high energy intensity of vCF production as the one for the base case. The sensitivity of vCF production energy requirement and sources accounts for the main impact on the full life cycle GHG emissions of vCF-based materials as shown in Figure 3 in main text.

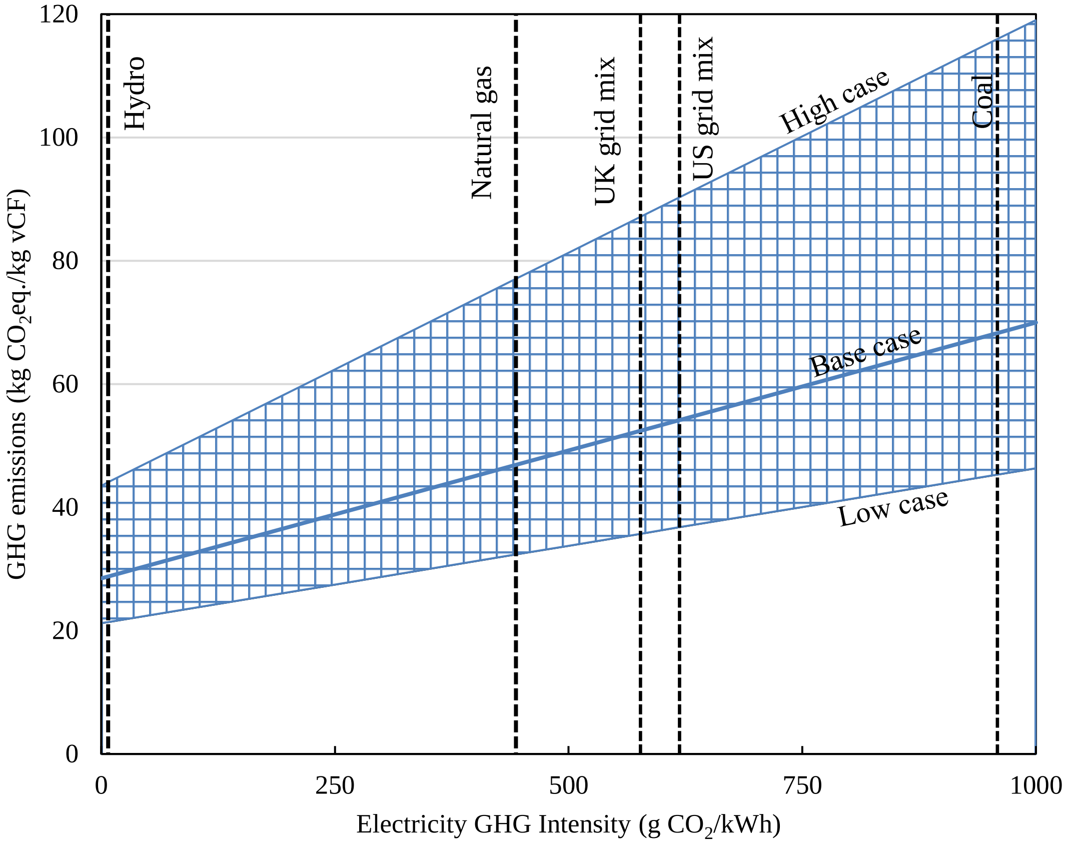

Figure S4. Sensitivity of GHG emissions to manufacture 1 kg vCF to the GHG intensity of grid electricity input. Note: UK grid mix is based on 2013 UK average (36% coal, 27% gas, 20% nuclear, 14.9% renewables and other sources; US grid mix is based on 2013 US average (38% hard coal, 27% gas, 19% nuclear, 13.3% renewables and other sources); natural gas generation is from a combined cycle facility. In the shaded areas, the bottom border line represents the low case of energy requirement of vCF production (198 MJ/kg), and the top border line represents the high case (595 MJ/kg) relative to the base case (the blue solid line in the middle).

Uncertainty in vehicle life does not alter the finding that rCFRP components achieve the lowest life cycle PED and GWP impact (see Figure S6). At extended vehicle lifetimes (up to 300,000 km), the advantages of lightweight materials become more pronounced. With increase of travel distances, the ability of rCFRP materials to reduce life cycle PED and GWP relative to steel increases. In particular, aligned rCFRP components reduce life cycle PED and GWP reductions in the region of 90% and 94% relative to steel. Conversely, shorter vehicle life reduces in-use fuel savings and is therefore detrimental to the performance of lightweight materials. Even so, rCF components can still reduce PED and GWP relative to conventional steel components. The traditional lightweight aluminium starts to show environmental benefits at a medium travelling life distance of about 150,000 km.

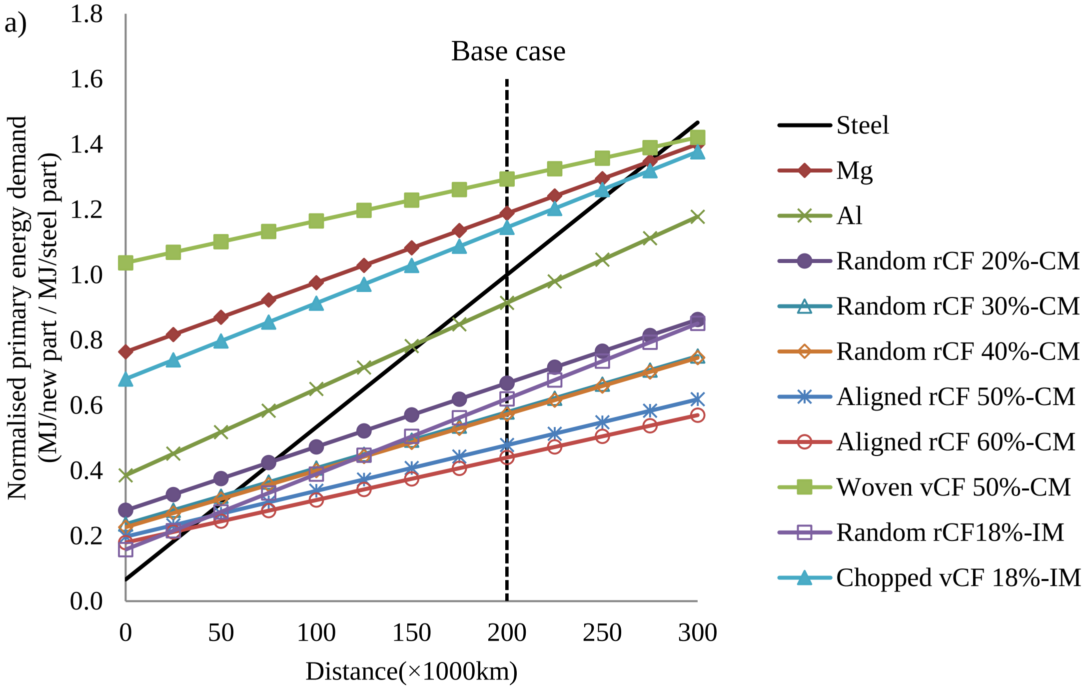

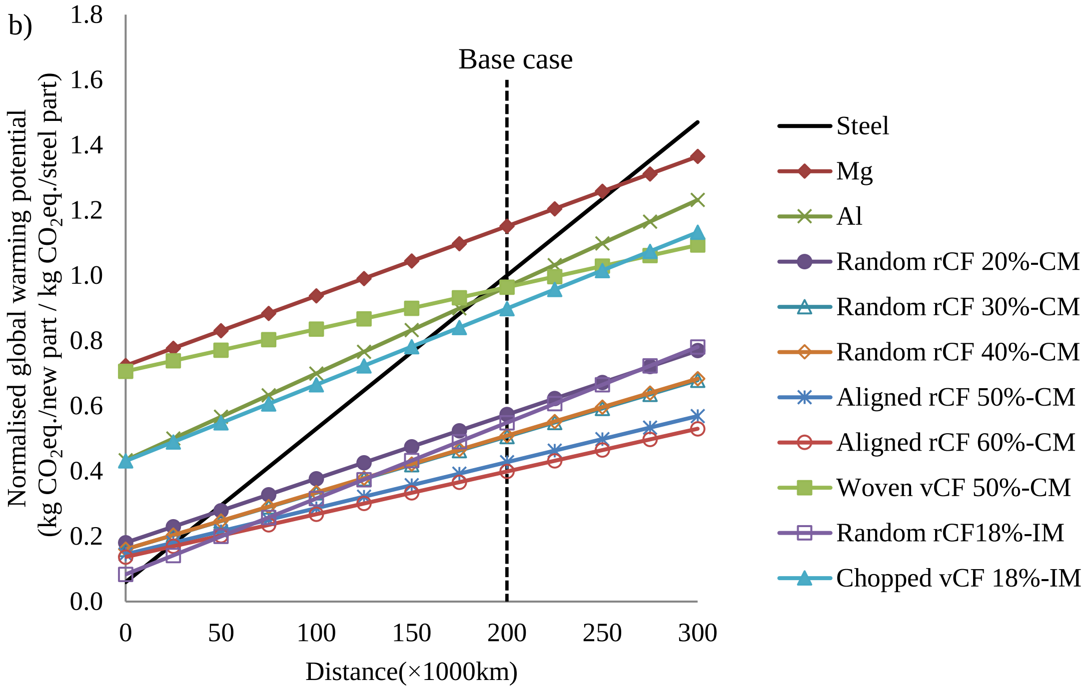

Figure S5. Sensitivity of a) life cycle PED (MJ/new part relative to MJ/steel part) and b) life cycle GHG emissions (kg CO_2eq./new part relative to kg CO_2eq./steel part) as a function of the vehicle distance travelled under λ=2.

Note: CM=compression moulding, IM=injection moulding

Uncertainty in vehicle fuel consumption considered for different brands of mid-size light duty vehicles with the value of 0.26-0.44 L/ (100km·100kg) similarly impact the performance of lightweight materials (see Figure S7). Life cycle GHG emissions of rCFRP materials are more sensitive to the mass induced fuel consumption than vCFRP material and lightweight aluminium. However, across the range of values considered, rCFRP materials are always favoured in reducing life cycle GHG emissions relative to steel among all materials considered in this study. It is also noted that woven vCFRP and aluminium could show significant GHG emission reduction for relatively high mass-induced fuel consumption assumed.

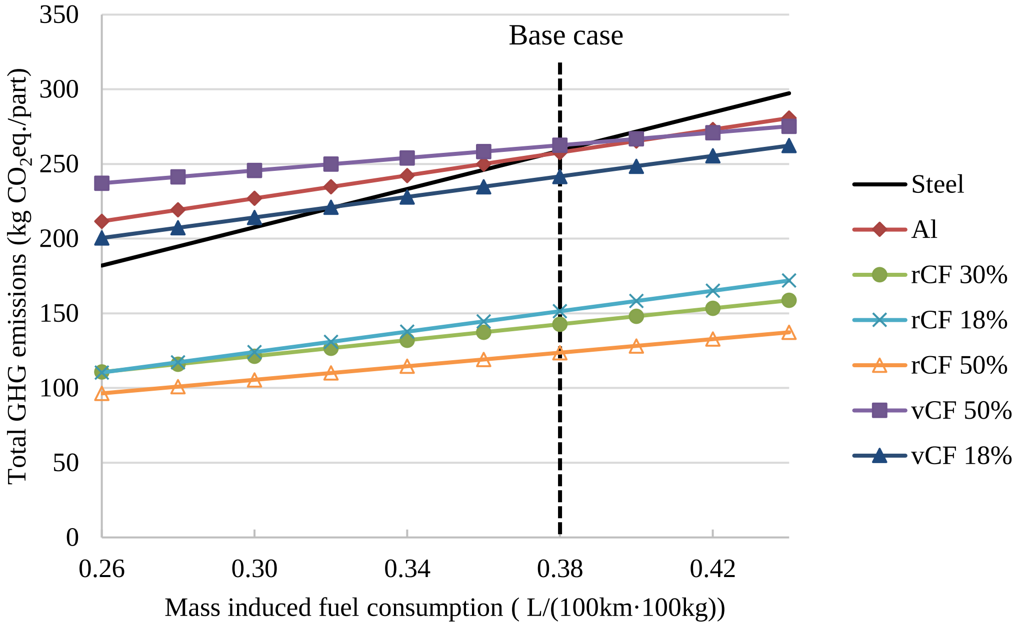

Figure S6. Sensitivity of total normalised GHG emissions with varied mass induced fuel consumption under λ=2

REFERENCES

(1) Wong, K. H., et al. The potential for fibre alignment in the manufacture of polymer composites from recycled carbon fibre. *SAE Int. J. Aerosp.* **2009,** *2* (2009-01-3237), 225-231.

(2) Wong, K. H., et al. Compression moulding of a recycled carbon fibre reinforced epoxy composite. In *SAMPE 2009 Conference*, Baltimore, Maryland, 2009.

(3) Witik, R. A., et al. Economic and environmental assessment of alternative production methods for composite aircraft components. *J. Clean. Prod.* **2012,** *29–30* (0), 91-102.

(4) Liu, Z., et al. Effect of fibre length and suspension concentration on alignment quality of discontinuous recycled carbon fibre. In *20th International Conference on Composite Materials*, Copenhagen, 2015.

(5) Strong, A. B. *Plastics: materials and processing*. Prentice Hall: 2006.

(6) Das, S. Life cycle assessment of carbon fiber-reinforced polymer composites. *Int. J. Life Cycle Assess.* **2011,** *16* (3), 268-282.

(7) European Commission-Intelligent Energy Europe Smithers Rapra Technology Ltd United Kingdom. *Reduced energy consumption in plastics engineering- European best practice guide*; 2006.

(8) Meng, F., et al. Energy and environmental assessment and reuse of fluidised bed recycled carbon fibres. *Compos. Part A-Appl. Sci. Manuf.* **2017,** *100*, 206-214.

(9) Suzuki, T.; Takahashi, J. *Prediction of energy intensity of carbon fiber reinforced plastics for mass-produced passenger cars*, In The Ninth Japan International SAMPE symposium, 2005; 2005; pp 14-19.

(10) Thiriez, A. An Environmental Analysis of Injection Molding. Master's Thesis. *Department of Mechanical Engineering* **2006**.

(11) Johannaber, F. *Injection molding machines*. 4th Edition ed.; Hanser Munich: 2008.

(12) Wong, K. H., et al. Effect of coupling agents on reinforcing potential of recycled carbon fibre for polypropylene composite. *Compos. Sci. Technol.* **2012,** *72* (7), 835-844.

(13) Polymer Nanostructures Lab of Penn State University. Injection moulding. <http://zeus.plmsc.psu.edu/>, (accessed January 2016).

(14) Weissman, A., et al. *A systematic methodology for accurate design-stage estimation of energy consumption for injection molded parts*, In Proceedings of the ASME 2010 International Design Engineering Technical Conference & Computers and Information Science in Engineering Conference, IDETC/CIE, 2010; 2010.

(15) Rao, N. S.; Schott, N. R. *Understanding Plastics Engineering Calculations: Hands-on Examples and Case Studies*. Carl Hanser Verlag GmbH Co KG: 2012.

(16) Krishnan, S., et al. *Sustainability Analysis and Energy footprint based Design in the Product Lifecycle*, In Indo-US Workshop on Designing Sustainable Products, Services and Manufacturing Systems, 2009; 2009.

(17) Krishnan, S., et al. *Machine level energy efficiency analysis in discrete manufacturing for a sustainable energy infrastructure*, In Infrastructure Systems and Services: Developing 21st Century Infrastructure Networks,(INFRA), 2009 Second International Conference on, 2009; IEEE: 2009; pp 1-6.

(18) Gutowski, T., et al. *Electrical energy requirements for manufacturing processes*, In 13th CIRP international conference on life cycle engineering, 2006; 2006.

(19) Ribeiro, I., et al. Assessment of energy consumption in injection moulding process. In *Leveraging Technology for a Sustainable World*, Springer: 2012; pp 263-268.

(20) Mattis, J., et al. *A framework for analyzing energy efficient injection-molding die design*, In Proceedings of the 1996 IEEE International Symposium on Electronics and the Environment. ISEE-1996, 1996; IEEE: 1996; pp 207-212.

(21) Kanungo, A.; Swan, E. All Electric Injection Molding Machines: How Much Energy Can You Save? In *13th Industrial Energy technology Conference*, New Orleans, LA, 2008.

(22) Madan, J., et al. Energy performance evaluation and improvement of unit-manufacturing processes: injection molding case study. *J. Clean. Prod.* **2014,** *105*, 157-170.

(23) Elduque, A., et al. *Sensitivity Analysis of the Environmental Impact of Polymer Injection Molding Process*, In The 4th World Sustainability Forum, 2014; Multidisciplinary Digital Publishing Institute: 2014.

(24) Sumitomo (SHI) Demag Plastics Machinery North America Inc. SYSTEC Hydraulic Series. <http://www.sumitomopm.com/previousspecs.html>, (accessed June 2016).

(25) Mitsubishi Heavy Industries Plastic Technology Co. Ltd. MMV series (large-sized injection molding machine). <http://www.mhi-pt.co.jp/injec_e/products/MMV/index.htm>, (accessed October 2016).

(26) Boothroyd, G., et al. *Product design for manufacture and assembly / Geoffrey Boothroyd, Peter Dewhurst, Winston Knight*. Marcel Dekker: 1994.

(27) Thiriez, A.; Gutowski, T. *An environmental analysis of injection molding*, In Electronics and the Environment, 2006. Proceedings of the 2006 IEEE International Symposium on, 2006; IEEE: 2006; pp 195-200.

(28) Spiering, T., et al. Energy efficiency benchmarking for injection moulding processes. *Robotics and Computer-Integrated Manufacturing* **2015**.

(29) Kent, R. Energy management in plastics processing—framework for measurement, assessment and prediction. *Plast. Rubber Compos.* **2008,** *37* (2-4), 96-104.

(30) Improve Your Plastic Injection Molding Business. Plastic Injection Molding Process - Energy Saving Techniques. <http://www.improve-your-injection-molding.com/>, (accessed December 2015).

(31) PlastiComp Inc. 30% Long Carbon Fiber Reinforced PP – Complēt LCF30-PP. <http://www.plasticomp.com/complet-lcf30-pp/>, (accessed June 2016).

(32) GoodFellow. Technical Information - Carbon/Epoxy Composite. <http://www.goodfellow.com/>, (accessed August 2016).

(33) Berthelot, J.-M. *Composite materials: mechanical behavior and structural analysis*. Springer Science & Business Media: New York, 2012.

(34) Daniel, I. M., et al. *Engineering mechanics of composite materials*. Oxford University Press New York: 1994; Vol. 3.

(35) MatWeb. Technical Data Sheet-AISI 1017 Steel, cold drawn. <http://www.matweb.com/>, (accessed July 2016).

(36) Kelly, J. C., et al. Impacts of Vehicle Weight Reduction via Material Substitution on Life-Cycle Greenhouse Gas Emissions. *Environ. Sci. Technol.* **2015,** *49* (20), 12535-12542.

(37) ASM Aerospace Specification Metals Inc. Aluminum 6061-T6. <http://asm.matweb.com/search/SpecificMaterial.asp?bassnum=MA6061t6>, (accessed December 2015).

(38) BMW GROUP. BMW i3 and i8 series car. <https://www.bmw.co.uk/en/index.html>, (accessed June 2016).

(39) Carberry, W. Airplane Recycling Efforts benefit boeing operators. *Boeing AERO Magazine QRT* **2008,** *4* (08), 6-13.

(40) Duflou, J. R., et al. Environmental impact analysis of composite use in car manufacturing. *CIRP Annals* **2009,** *58* (1), 9-12.

(41) Witik, R. A., et al. Carbon fibre reinforced composite waste: An environmental assessment of recycling, energy recovery and landfilling. *Compos. Part A-Appl. Sci. Manuf.* **2013,** *49*, 89-99.